BIOLOGY OF REPRODUCTION (2014) **90**(4):84, 1–15
Published online before print 19 March 2014.
DOI 10.1095/biolreprod.113.114637

Arginine Decarboxylase and Agmatinase: An Alternative Pathway for De Novo Biosynthesis of Polyamines for Development of Mammalian Conceptuses[1]

Xiaoqiu Wang,[4,5] Wei Ying,[4,5] Kathrin A. Dunlap,[4,5] Gang Lin,[3,5] M. Carey Satterfield,[4,5] Robert C. Burghardt,[6] Guoyao Wu,[4,5] and Fuller W. Bazer[2,4,5]

[4]*Center for Animal Biotechnology and Genomics, Texas A&M University, College Station, Texas*
[5]*Department of Animal Science, Texas A&M University, College Station, Texas*
[6]*Department of Veterinary Integrative Biosciences, Texas A&M University, College Station, Texas*

ABSTRACT

Ornithine decarboxylase (ODC1) is considered the rate-controlling enzyme for the classical de novo biosynthesis of polyamines (putrescine, spermidine, and spermine) in mammals. However, metabolism of arginine to agmatine via arginine decarboxylase (ADC) and conversion of agmatine to polyamines via agmatinase (AGMAT) is an alternative pathway long recognized in lower organisms, but only recently suggested for neurons and liver cells of mammals. We now provide evidence for a functional ADC/AGMAT pathway for the synthesis of polyamines in mammalian reproductive tissue for embryonic survival and development. We first investigated cellular functions of polyamines by in vivo knockdown of translation of mRNA for ODC1 in ovine conceptus trophectoderm using morpholino antisense oligonucleotides (MAOs) and found that one-half of the conceptuses were morphologically and functionally either normal or abnormal. Furthermore, we found that increases in ADC/AGMAT mRNA levels and in the translation of *AGMAT* mRNA among conceptuses in MAO-ODC1 knockdown compensated for the loss of ODC1, supporting polyamine synthesis from arginine and accounting for the normal and abnormal phenotypes of conceptuses. We conclude that the majority of polyamine synthesis is by the conventional ODC1-dependent pathway (arginine-ornithine-putrescine) and that deficiencies in ODC1 result in increased activity of the rescue ADC/AGMAT-dependent pathway (arginine-agmatine-putrescine) for production of polyamines. The presence of an alternative ADC/AGMAT pathway for converting arginine into putrescine is functionally important for supporting survival and development of mammalian conceptuses.

agmatine, development, polyamines, sheep, trophectoderm

INTRODUCTION

Embryonic mortality is a major constraint to reproductive performance in all mammalian species [1]. Estimates of embryonic death in sheep, other ruminants, and most mammals range from 20% to 40%, with two-thirds of those losses occurring during the peri-implantation period of pregnancy [1, 2]. Successful establishment and maintenance of pregnancy requires appropriate development of the conceptus (embryo/fetus and its extraembryonic membranes) for pregnancy recognition signaling (e.g., interferon tau [IFNT] in ruminants, estrogen in pigs, placental lactogen or prolactinlike hormones in rodents, and chorionic gonadotrophin in primates) required for maintenance of the corpus luteum (CL) that secretes progesterone [1, 2]. Progesterone is required for an intrauterine environment that supports implantation, placentation, and uterine functions essential for birth of healthy offspring [1, 2]. During the peri-implantation period of pregnancy in ungulates and cetaceans, the conceptus undergoes dramatic morphological transitions from spherical to tubular to filamentous forms immediately prior to implantation [1, 2]. This process is highly dependent on the composition of histotroph. Histotroph includes secretions from uterine luminal (LE), superficial glandular (sGE), and glandular (GE) epithelia as well as selective transport of nutrients into the uterine lumen, including enzymes, growth factors, adhesion proteins, cytokines, hormones, transport proteins, amino acids, and glucose. Arginine, a nutritionally essential amino acid for conceptus survival and development [3], increases 13-fold in ovine uterine histotroph between Days 10 to 15 of pregnancy [4]. Arginine is transported into conceptuses via its major transporter SLC7A1, that is, solute carrier family 7, (cationic amino acid transporter, y+ system), member 1 [5], and can be metabolized to either nitric oxide (NO) via NO synthase (mainly the endothelial isoform NOS3) [6] or the polyamine putrescine via ornithine decarboxylase (ODC1). Furthermore, putrescine is metabolized to spermidine and spermine [6]. NO is essential for vasodilation and angiogenesis in the pregnant uterus to regulate uteroplacental-fetal blood flows and transfer of nutrients and oxygen from mother to fetus [7–10]. Polyamines are key regulators of DNA [11–13] and protein synthesis, scavengers of reactive oxygen species [14], cell proliferation [15–17] via the mechanistic target of rapamycin cell-signaling pathway, and differentiation of tissues [16, 18]. Thus, polyamines support survival, growth, and development of the conceptus during the peri-implantation period of pregnancy, and depletion of cellular polyamines prevents translation of mRNAs and growth of mammalian cells [19] as well as conceptuses [20–22].

The conventional pathway from arginine to polyamines is via arginase and ODC1 in mammalian tissues [20–22]; however, there is recent evidence suggesting an alternative pathway for synthesis of polyamines in mammals that is well known for lower organisms [23, 24]. The alternate pathway is the arginine-agmatine-polyamine pathway that requires conversion of arginine to agmatine by arginine decarboxylase (ADC) followed by conversion of agmatine to putrescine via agmatinase (AGMAT). This pathway may exist in nervous

[1]Supported by Agriculture and Food Research Initiative Competitive Grants No. 2011-6705-20028 from the USDA National Institute of Food and Agriculture.
[2]Correspondence: E-mail: fbazer@cvm.tamu.edu
[3]Current Address: State Key Laboratory of Animal Nutrition, China Agricultural University, Beijing, China 100193.

Received: 3 October 2013.
First decision: 25 November 2013.
Accepted: 11 March 2014.

eISSN: 1529-7268 http://www.biolreprod.org
ISSN: 0006-3363

tissue [24] and liver [23] of rats. When one queries GeneCardV3 (http://www.genecards.org/) [25], expression in the ovary, uterus, and placenta is indicated; however, there are no published reports of expression of the ADC/AGMAT pathway in the female reproductive tract or conceptus tissues although polyamines are pivotal for diverse functions in the mammalian reproductive tract. Therefore, we conducted experiments in 2011 and 2012 to elucidate the consequences of knockdown of translation of *ODC1* mRNA and to test the hypothesis that the ADC/AGMAT pathway is activated to compensate for a deficiency in ODC1 protein and ensure synthesis of polyamines to support embryonic survival and development in our ovine model. We found similar results in both years in that in vivo knockdown of translation of *ODC1* in ovine conceptuses results in two distinct phenotypes of conceptuses: a morphologically and functionally normal phenotype and a morphologically and functionally abnormal phenotype. There was a compensatory increase in abundance of AGMAT protein in conceptuses with a normal phenotype and lack of such compensation in conceptuses with an abnormal phenotype. Specifically, some conceptuses were rescued by compensatory increase of de novo polyamine synthesis via metabolism of arginine to agmatine and putrescine following in vivo morpholino loss-of-function of ODC1 [26]. Furthermore, we examined the metabolism of arginine to agmatine via ADC/AGMAT in normal conceptuses during the peri-implantation period of pregnancy, and this confirmed the presence of this pathway in ovine conceptuses during the peri-implantation period of pregnancy.

MATERIALS AND METHODS

Morpholino Design

Morpholino antisense oligonucleotides (MAOs) were designed and synthesized to inhibit translational initiation of the mRNAs for *ODC1*, an enzyme involved in polyamine synthesis, and a 5′-scrambled morpholino to serve as a MAO control (Gene Tools). Briefly, the MAO-ODC1 had the sequence 5′-ACTCT TCATT ACCAA AGTTG TTCAT-3′ and targeted the starting codon of *ODC1* mRNA (GenBank accession no. NM_002539), whereas the MAO control had the sequence 5′-CCTCT TACCT CAGTT ACAAT TTATA-3′ and targeted a splice site mutant of *Homo sapiens* hemoglobin β-chain (*HBB*) gene (GenBank accession no. GU324922). All the morpholinos were synthesized with a 3′-lissamine modification (red color) for convenient detection of cellular uptake.

Animal Model

Mature Rambouillet ewes (*Ovis aries*) were observed daily for estrus (Day 0 is day of onset of estrus) in the presence of vasectomized rams and used in experiments only after they had exhibited at least two estrous cycles of normal duration (16–18 days). All the experimental and surgical procedures were in compliance with the Guide for the Care and Use of Agriculture Animals in Research Teaching and approved by the Institutional Animal Care and Use Committee of Texas A&M University.

Experimental Design and Tissue Collection

Study one. At estrus, ewes (n = 20) were mated to an intact ram of proven fertility. On Day 8 postmating, the base of the uterine horn ipsilateral to the CL of ewes that had not returned to estrus (n = 7 MAO control and 8 MAO-ODC1) was double ligated to prevent migration of the conceptus into the contralateral uterine horn. This procedure does not affect development or implantation of ovine conceptuses [26]. MAO-ODC1 or MAO control (100 nmol) was complexed with Gene Tools Endo-Porter delivery reagent (100 μl) and diluted to 1 ml final volume with OPTI-MEM (Invitrogen), and injected into the lumen of the ipsilateral uterine horn with respect to the location of the CL. On Day 16, ewes were ovariohysterectomized to obtain conceptuses and subjected to uterine flushing to obtain uterine tissues from the treatment groups: MAO-ODC1 (n = 8), and MAO control (n = 7). Briefly, the ligated uterine horn ipsilateral to CL was flushed with 10 ml of sterile phosphate-buffered saline (PBS), pH 7.2. Pregnancy rates were recorded based on the presence or absence of a functional CL and the presence of a conceptus in the uterine flushing. If a conceptus was present, its morphology was recorded as small, thin, fragile, fragmented, elongated, and/or healthy. After photographing each conceptus using a digital camera, the conceptus was immediately removed from the uterine flush with a transfer pipette, and the recovered volume of uterine flush recorded. Portions of the conceptus were then placed in optimal-cutting temperature compound (Miles), frozen in liquid nitrogen, and stored at −80°C. Another portion of the conceptus was fixed in freshly prepared 4% (wt/vol) paraformaldehyde in PBS, pH 7.2, for 24 h and then in 70% ethanol for 24 h. The fixed tissues were dehydrated through a graded series of alcohol to xylene and embedded in Paraplast-Plus (Oxford Labware). The remaining conceptus tissue was frozen in liquid nitrogen and stored at −80°C. Sections (~0.5 cm) from the midportion of each ligated uterine horn ipsilateral to the CL were fixed in fresh 4% paraformaldehyde for eventual embedding in Paraplast-Plus (Sigma). The uterine flush was clarified by centrifugation (5000 × *g* for 15 min at 4°C), aliquoted, and stored at −80°C until analyzed. This study was performed with the same number of ewes and treatments in two consecutive breeding seasons in 2011 and 2012.

Study two. At estrus (Day 0), ewes were mated to an intact ram of proven fertility and assigned randomly to be ovariohysterectomized on Day 12, 13, 14, 15, or 16 of pregnancy (n = 5–6 ewes per day and status) as described previously [27]. Pregnancy was confirmed by the presence of a morphologically normal conceptus and a functional CL. On each day of pregnancy studied, the two uterine horns were flushed with 20 ml of sterile PBS, pH 7.2, because of the presence of conceptus tissue in both uterine horns. If the conceptus was present, its morphology was recorded as previously described (spherical, tubular, or filamentous) and the recovered volume of the uterine flush was recorded. Photographs of the conceptus were obtained using a digital camera. Conceptuses were frozen in liquid nitrogen and stored at −80°C. The uterine flush was clarified by centrifugation (5000 × *g* for 15 min at 4°C), aliquoted, and stored at −80°C.

Study three. Ewes were mated to either an intact or a vasectomized ram when detected in estrus (Day 0) and 12 and 24 h later. On Days 10, 12, 14, or 16 of the estrous cycle and Day 10, 12, 14, or 16 of pregnancy (n = 4–10 ewes per day and status), uteri were flushed with 20 ml of sterile PBS, pH 7.2, as described previously. Sections (~0.5 cm) from the midportion of uterine horn ipsilateral to the CL were fixed in fresh 4% paraformaldehyde for eventual embedding in Paraplast-Plus (Sigma). The uterine flush was clarified by centrifugation (5000 × *g* for 15 min at 4°C), aliquoted, and stored at −80°C until analyzed.

Radioimmunoassay Analyses of IFNT

The amount of IFNT in the uterine flush was quantified by radioimmunoassay (RIA), which was developed at Colorado State University using recombinant ovine IFNT (roIFNT) protein and anti-roIFNT polyclonal antibody (1:60 000) from Dr. Fuller W. Bazer (Texas A&M University) [28]. Anti-rabbit gamma globulin was used as the second antibody (generated at Colorado State University) and was diluted at 1:25. Recombinant oIFNT was radioiodinated with ^{125}I using a chloramine T procedure and purified using Sephadex (G25; GE Health Care) column chromatography. Uterine flushings were initially diluted 1:50 in 0.1% PBS gel and analyzed in the RIA. In the event that IFNT was not detected in diluted samples, uterine flushes were examined in the RIA again without being diluted. Anti-roIFNT antibody was added to uterine flushing samples, vortexed, and incubated at 4°C for 24 h. Radioactive roIFNT was added, vortexed, and incubated for 24 h at 4°C followed by incubation at 4°C for 72 h with secondary anti-rabbit gamma globulin antibody. The assay was then terminated with 3 ml of cold PBS and centrifuged at 2800 rpm for 30 min. The supernatant was removed, and the radioactivity of the pellet was determined using a gamma counter. This RIA was optimized for detection of roIFNT in uterine flushings at a sensitivity of 0.1 ng/ml and a range of detection of 0.1 to 13 ng/ml. The intra- and interassay coefficients of variation were 6.2% and 4.0%, respectively.

Histological Analyses of Conceptus Morphology

The conceptuses embedded in paraffin were sectioned (~5 μm) and mounted on glass slides for staining with hematoxylin and eosin as described previously [5]. The morphology of each tissue sample was examined, and images were captured using an Axioplan 2 microscope with Axiocam HR digital camera and Axiovision 4 software.

Immunohistochemical Analyses

Immunohistochemical localization of ODC1, NOS3, SLC7A1, ADC, and AGMAT proteins in ovine uteri or conceptuses was performed as described

previously [6] in tissue sections of uteri (~10 μm) and conceptuses (~5 μm) with rabbit anti-ODC1 polyclonal immunoglobulin G (IgG) (ab97395; Abcam), mouse anti-NOS3 monoclonal IgG (610297; BD Transduction Laboratories), rabbit anti-SLC7A1 polyclonal IgG (ab37588; Abcam), rabbit anti-ADC polyclonal IgG (HPA028045; Sigma-Aldrich), and rabbit anti-AGMAT polyclonal IgG (ab85172; Abcam) at a dilution of 1:500, 1:250, 1:250, 1:50, and 1:100, respectively. Antigen retrieval was performed using boiling 0.01 M sodium citrate buffer, pH 6.0, for ODC1 and NOS3 proteins, and protease (0.5 mg/ml in PBS) for SLC7A1 protein. Purified nonrelevant rabbit or mouse IgG was used as a negative control to replace the primary antibody at the same final concentration. Immunoreactive protein was visualized in sections using the VECTASTAIN ABC Kit (PK-6101 for rabbit IgG and PK-6102 for mouse IgG; Vector Laboratories) following the manufacturer's instructions and 3,3′-diaminobenzidine tetrahydrochloride (D5637; Sigma-Aldrich) as the color substrate. Sections were not counterstained before affixing the coverslips.

Quantitative Immunofluorescence Microscopy

Effective delivery of the lissamine-labeled MAOs was analyzed by fluorescence microscopy. Cryosections of the conceptuses (~8 μm) as well as uteri (~12 μm) were prepared, directly followed by a mounting medium containing 4′,6-diamidino-2-phenylindole (DAPI) to visualize the nuclei [26]. Also, the translational knockdown efficiency of ODC1 and its effects on NOS3, SLC7A1, ADC, and AGMAT proteins were evaluated in frozen sections of conceptuses or uteri by immunofluorescence microscopy as previously described [17, 29, 30]. Briefly, the cryosections were fixed in cold methanol for 10 min at −20°C. After removal of the optimal-cutting temperature compound and rinsing with 0.02 M of PBS containing 0.3% Tween, the sections were blocked in 5% normal goat serum (i.e., 1:10 dilution) for 2 h at room temperature, rinsed, and then incubated with primary antibody overnight at 4°C. Primary antibodies included rabbit anti-ODC1 polyclonal IgG (ab97395; Abcam), mouse anti-NOS3 monoclonal IgG (610297; BD Transduction Laboratories), rabbit anti-SLC7A1 polyclonal IgG (ab37588; Abcam), rabbit anti-ADC polyclonal IgG (HPA028045, Sigma-Aldrich), and rabbit anti-AGMAT polyclonal IgG (ab85172; Abcam) at dilutions of 1:500, 1:250, 1:250, 1:50, and 1:100, respectively. Purified nonrelevant rabbit or mouse IgG was substituted for the primary antibody as a negative control. Sections probed with primary antibody were incubated with goat anti-rabbit IgG Alexa 488 (Chemicon) at 1:250 dilution for 1 h at room temperature, and then rinsed in 0.02 M of PBS containing 0.3% Tween and overlaid with Prolong Gold Antifade with DAPI. Slides were stored at 4°C in the dark before microscopic analysis. Fluorescence images of conceptuses were captured using an Axioplan 2 microscope with an Axiocam HR camera and Axiovision 4 software (Carl Zeiss). For each primary antibody, images were captured with identical microscope and detector settings to facilitate comparisons of spatial distribution and fluorescence intensity among the treatments. To ensure specificity of signals and absence of fluorescence bleed-through, sections were examined with fluorescence filter sets at longer and shorter wavelengths. Sections from conceptuses or uteri in all the treatment groups were analyzed in duplicate in the same run, with three sections per conceptus or uterus and five fields per section. Signals were quantified by Image J software (Version 1.47, National Institutes of Health) using standardized procedure as described previously [31].

Western Blot Analyses of Knockdown Efficiency of ODC1 Protein in Ovine Trophectoderm Cells

An established mononuclear ovine trophectoderm (oTr) cell line from Day 15 conceptuses was used in the present in vitro studies as described previously [17]. The oTr cells were cultured in Dulbecco-modified Eagle medium-F12 that included 10% fetal bovine serum (Gibaco BRL), 50 units/ml penicillin, 50 μg/ml streptomycin, 0.1 mM nonessential amino acids, 1 mM sodium pyruvate, 2 mM glutamine, and 4 μg/ml insulin. When the density of cells in the dishes reached about 80% confluence, they were split into three dishes for culture, and frozen stocks of cells were prepared at each passage. For Western blot analyses, monolayer cultures of oTr cells (between passage 9 and 13) were seeded at 50 000 cells/ml medium (5 ml per dish, three dishes per group) in 60 mm cell culture dishes (430166; Fisher Scientific). After reaching 80% confluence, oTr cells were washed with PBS and incubated with Endo-Porter aqueous delivery reagent (Gene Tools) (8 μl/ml medium) and 20 μM MAO-ODC1 or MAO control. After 48 h, transfected cells were lysed for 30 min at 4°C in 0.3 ml of a buffer consisting of 1% Triton X-100, 0.5% Igepal CA-630, 150 mM NaCl, 10 mM Tris-HCl (pH 7.6), 1 mM ethylenediaminetetraacetic acid, 1 mM ethylene glycol tetraacetic acid, 0.2 mM Na_3VO_4, and protease inhibitor cocktail, including 0.2 mM phenylmethylsulfonyl fluoride, 50 mM NaF, 30 mM $Na_4P_2O_7$, 1 μg/ml leupeptin, and 1 μg/ml pepstatin (1 tablet in 50 ml; 11 873 580 001; Roche). Cell lysates were passed through a 26-gauge needle and clarified by centrifugation (21 000 × *g* for 15 min at 4°C). Protein concentration in the supernatant fluid was determined using the Bradford protein assay (Bio-Rad) with bovine serum albumin as the standard. Proteins were denatured, separated using SDS-PAGE (4% to 12% gradient gel at 150 V for 2.5–3 h), and transferred to nitrocellulose membrane overnight (~16 h) at 20 V using the Bio-Rad Transblot (Bio-Rad). Membranes were blocked in 5% fat-free milk in 20 mM Tris, 150 mM NaCl, pH 7.5, and 0.1% Tween-20 (TBST) for 3 h and then incubated with primary antibodies at 4°C overnight with gentle rocking. After washing three times with TBST, the membranes were incubated at room temperature for 2 h with secondary antibody. The primary antibody, rabbit anti-ODC1 polyclonal IgG (ab97395; Abcam), and secondary antibody, horseradish peroxidase-linked anti-rabbit IgG (Cell Signaling), were used at dilutions of 1:500 and 1:10 000, respectively. The membranes were then washed with TBST, followed by development using enhanced chemiluminescence detection (SuperSignal West Pico) according to the manufacturer's instructions. As a loading control, rabbit anti-β-actin (ACTB) polyclonal IgG (1:5000 dilution; ab8227; Abcam) was used after detecting the proteins on the blots. Multiple exposures of each Western blot were performed to ensure linearity of chemiluminescent signals. Western blots were quantified by measuring the intensity of light emitted from correctly sized bands under ultraviolet light using a ChemiDoc EQ system and Quantity One software (Bio-Rad).

RNA Isolation and Quantitative Real-Time PCR Analyses

Total RNA was isolated from ovine conceptuses using Trizol (Invitrogen) according to manufacturer's instructions. The quantity and quality of total RNA were determined by spectrometry (wavelength = 230 nm) and by denaturing agarose gel electrophoresis, respectively. Total RNA samples were digested with RQ1 RNase-Free DNase (Promega) and subsequently cleaned up using a RNeasy Mini Kit (Qiagen). The levels of mRNA encoding *ADC* and *AGMAT* genes in ovine conceptuses were determined by quantitative real-time polymerase chain reaction. For *ADC*, forward (5′-TCCCTGCCTCTA GAAGCTCACT-3′) and reverse (5′-ATCGTTTCCACTCCGGATAGAC-3′) primers were derived from the bovine *ADC* mRNA coding sequence (GenBank accession No. NM_001038510). For *AGMAT*, forward (5′-TCTCTTCAAGCT GACCCACCAT-3′) and reverse (5′-TCACGCCTTCACTGCAGATT-3′) primers were derived from the bovine *AGMAT* mRNA coding sequence (GenBank accession No. XM_002694143). Primer specificity and efficiency were determined by the addition of a dissociation curve step to the RT reaction and through the generation of a standard curve using known quantities of conceptus cDNA, respectively. Only those primers amplifying a single product and determined to be between 97.5% and 102.5% efficient were utilized for quantitative analyses. First-strand cDNAs were synthesized from 1 μg of total RNA using oligo (deoxythymidine) primers, random hexamer primers, and SuperScript II Reverse Transcriptase. Quantitative PCR was performed using the ABI prism 7900HT system (Applied Biosystems) with Power SYBR Green PCR Master Mix (Applied Biosystems) as specified by the manufacturer. Each individual sample was run in triplicate using the following conditions: 50°C for 2 min, 95°C for 10 min, followed by 40 cycles of 95°C for 15 sec and 60°C for 30 sec. A dissociation curve was generated to determine amplification of a single product. The threshold line was set at the linear region of the plots above the baseline noise, and threshold cycle (C_T) values were determined at the cycle number at which the threshold line crossed the amplification curve. Ovine alpha-tubulin (*TUBA*, GenBank accession No. AF251146.1) was used as reference gene with forward (5′- GGTCTTCAAGGCTTCTTGGT-3′) and reverse (5′- CATAATCGACAGAGAGGCGT-3′) primers. The abundance of ADC and AGMAT mRNAs was calculated using the comparative Ct method.

Analyses for Putrescine, Spermidine, Spermine, Agmatine, and Amino Acids

Concentrations of polyamines as well as agmatine and amino acids were determined in uterine flushes and conceptuses using the modified procedures described by Wu et al. [32–34]. Briefly, uterine flushes (100 μl) or conceptuses (~20 mg) were acidified with 200 μl of 1.5 M $HClO_4$ and neutralized with 100 μl of 2 M K_2CO_3. The neutralized extracts (for polyamines and agmatine, 1:5 dilution for conceptuses and no further dilution for uterine flushes; for amino acids, 1:25 dilution for both conceptuses and uterine flushes) were used for analysis by an high-performance liquid chromatography method involving precolumn derivatization with o-phthaldialdehyde (OPA) reagent I or II. OPA reagent I (for polyamines and agmatine) was prepared by dissolving 50 mg OPA and 50 mg N-acetyl-L-cysteine in 1.25 ml methanol, followed by addition of 11.2 ml of 0.04 M sodium borate buffer, pH 9.5, and 0.4 ml of Brij-35. OPA reagent II (for amino acids) was prepared by dissolving 50 mg OPA in 1.25 ml methanol, followed by addition of 11.2 ml of 0.04 M sodium borate, pH 9.5, 50

μl 2-mercaptoethanol, and 0.4 ml Brij-35. The assay mixture contained 100 μl sample and 100 μl of 1.2% benzoic acid (in 40 mM sodium borate, pH 9.5). An aliquot (100 μl) of assay mixture was derivatized in an autosampler (model 712 WISP; Waters) with 100 μl of 30 mM OPA reagent I or II, and 100 μl of the derivatized mixture was injected in a Supelco 3-μm reversed-phase C_{18} column (150 × 4.6 mm inner diameter). Polyamines, agmatine, or amino acids were separated using a solvent gradient consisting of solution A (0.1 M sodium acetate, 2 mM SDS, 0.5% tetrahydrofuran, and 9% methanol, pH 7.2) and solution B (methanol and 2 mM SDS). Putrescine, spermidine, spermine, agmatine, as well as amino acids in the samples were quantified on the basis of authentic standards.

Statistics

Normality of data and homogeneity of variance were tested using the Shapiro-Wilk test and Brown-Forsythe test in Statistical Analysis System, respectively (version 8.1; SAS Institute). Data in each of the three studies were analyzed by least-squares one-way analysis of variance (ANOVA) and post hoc analysis (the Fisher least significant difference) with each ewe/conceptus as an experimental unit. The effect of treatment on pregnancy rates was analyzed using chi-square. All the analyses were performed using SAS. Data are expressed as means with SEM. $P < 0.05$ was considered significant.

RESULTS

In Vivo Knockdown of ODC1 Translation in Trophectoderm of Ovine Conceptuses Results in Morphologically and Functionally Normal Conceptuses and Morphologically and Functionally Abnormal Phenotypes

Polyamines support embryonic survival, growth, and development, and ODC1 is the rate-controlling enzyme for de novo synthesis of polyamines in the conventional pathway in which arginine is converted to ornithine by arginase and ornithine is converted to putrescine by ODC1. Therefore, we investigated in vivo translational knockdown of ODC1 protein in ovine conceptus trophectoderm (Tr) to determine its effect on growth and development of the conceptus. An MAO to *ODC1* mRNA tagged with 3′-lissamine (red color) was designed to inhibit translation of *ODC1* mRNA (MAO-ODC1) in ovine conceptuses. On Day 8 postmating, either MAO-ODC1 (n = 8) or MAO control (n = 7) was injected into the uterine lumen, and conceptuses were obtained for morphological and molecular analyses on Day 16 of pregnancy. Interestingly, there were two phenotypes of conceptuses in response to MAO-ODC1 as compared to MAO control conceptuses that were morphologically and functionally normal filamentous conceptuses. In both 2011 and 2012, half (n = 4) of the MAO-ODC1 treated conceptuses were morphologically and functionally normal, designated here as MAO-ODC1(a), whereas the other half (n = 4) were morphologically and functionally abnormal (small, not filamentous, and fragmented), and designated here as MAO-ODC1(b) (Fig. 1A). Because of the morphology of these conceptuses, it was not possible to assess differences in their length or other gross measures of development. However, histological analysis revealed that, as compared to MAO control conceptuses, the Tr and extraembryonic endoderm (En) were well organized in the MAO-ODC1(a) group, whereas Tr and En were disorganized and fragmented in MAO-ODC1(b) conceptuses (Fig. 1B). As a measure of conceptus functional competency, we assessed the total amount of IFNT (volume of uterine flushing × concentration of IFNT), the pregnancy recognition signal in ruminants, in the uterine flushings and detected no difference between MAO-ODC1(a) and MAO control, but there was less IFNT ($P < 0.01$) in uterine flushes from the MAO-ODC1(b) group (Fig. 1C). There were no statistically significant differences in pregnancy rates (Fig. 1D), volumes of uterine flushes recovered (Fig. 1E), or total recoverable protein in uterine flushes (Fig. 1F) due to phenotype of conceptus or between MAO control and MAO-ODC1 treatment groups. These results indicate that knockdown of ODC1 creates two phenotypes of conceptuses, half were rescued to normal development and the other half were not rescued, failed to elongate and develop normally, and produced less IFNT.

MAO Delivery and Knockdown Effect of ODC1 Protein in Ovine Conceptuses

We evaluated efficiencies for MAO delivery and knockdown of ODC1 translation by immunofluorescence microscopy. The red colored 3′-lissamine tag in MAOs (Fig. 2A) confirmed MAO uptake by conceptus Tr (Fig. 2G). Furthermore, knockdown ($P < 0.01$) of ODC1 protein was confirmed in MAO-ODC1(a) and MAO-ODC1(b) conceptuses as compared with MAO control conceptuses by immunofluorescence (Fig. 2, B and H) and immunohistochemistry (Fig. 2C), as well as in MAO-ODC1 treated oTr cells compared with MAO control by Western blot analysis (Fig. 2F). There were no differences in ODC1 protein in uterine LE, sGE, and GE as expected because these cells do not take up MAOs (Fig. 2, D and E). These results indicated that MAOs were efficiently delivered into conceptuses and that successful knockdown of ODC1 protein was achieved in conceptuses of both MAO-ODC1(a) and MAO-ODC1(b).

In Vivo Knockdown of ODC1 Partially Suppressed Expression of NOS3 Protein Without Affecting Expression of SLC7A1 Protein in Ovine Conceptuses

Besides polyamine synthesis, arginine can be metabolized to form citrulline and NO mainly via NOS3 in ovine conceptuses during the peri-implantation period of pregnancy [6]. Therefore, we compared the abundance of NOS3 protein in conceptuses of all the treatment groups. Notably, NOS3 was less abundant ($P < 0.01$) in MAO-ODC1(b) conceptuses, but there was no difference ($P > 0.05$) in NOS3 protein between MAO-ODC1(a) and MAO control conceptuses (Fig. 3, A, C, and E). Also, because arginine is transported from the uterine lumen mainly by SLC7A1 into ovine conceptuses during the peri-implantation period of pregnancy [5], we compared the abundance of SLC7A1 protein in conceptuses of all the treatment groups. The results indicated that there were no differences ($P > 0.05$) in SLC7A1 protein in conceptuses among the treatment groups (Fig. 3, B, D, and F).

In Vivo Knockdown of ODC1 Reduces Polyamines and Increases Ornithine and Citrulline in the Uterine Lumen and Differentially Affects Its De Novo Synthesis in Conceptuses via Conversion of Ornithine to Putrescine

To examine whether the downstream products of ornithine metabolism were affected by knockdown of ODC1 protein, the abundance of polyamines (i.e., putrescine, spermidine, and spermine) in the uterine lumen and in conceptuses were analyzed for all the ewes. Putrescine, spermidine, and spermine were less abundant ($P < 0.05$) in uterine flushings from both MAO-ODC1(a) and MAO-ODC1(b) as compared with MAO controls (Fig. 4A). However, within conceptus tissues, the abundance of polyamines was not different between MAO-ODC1(a) and MAO control conceptuses (Fig. 4B), but decreased ($P < 0.01$) in MAO-ODC1(b) conceptuses as

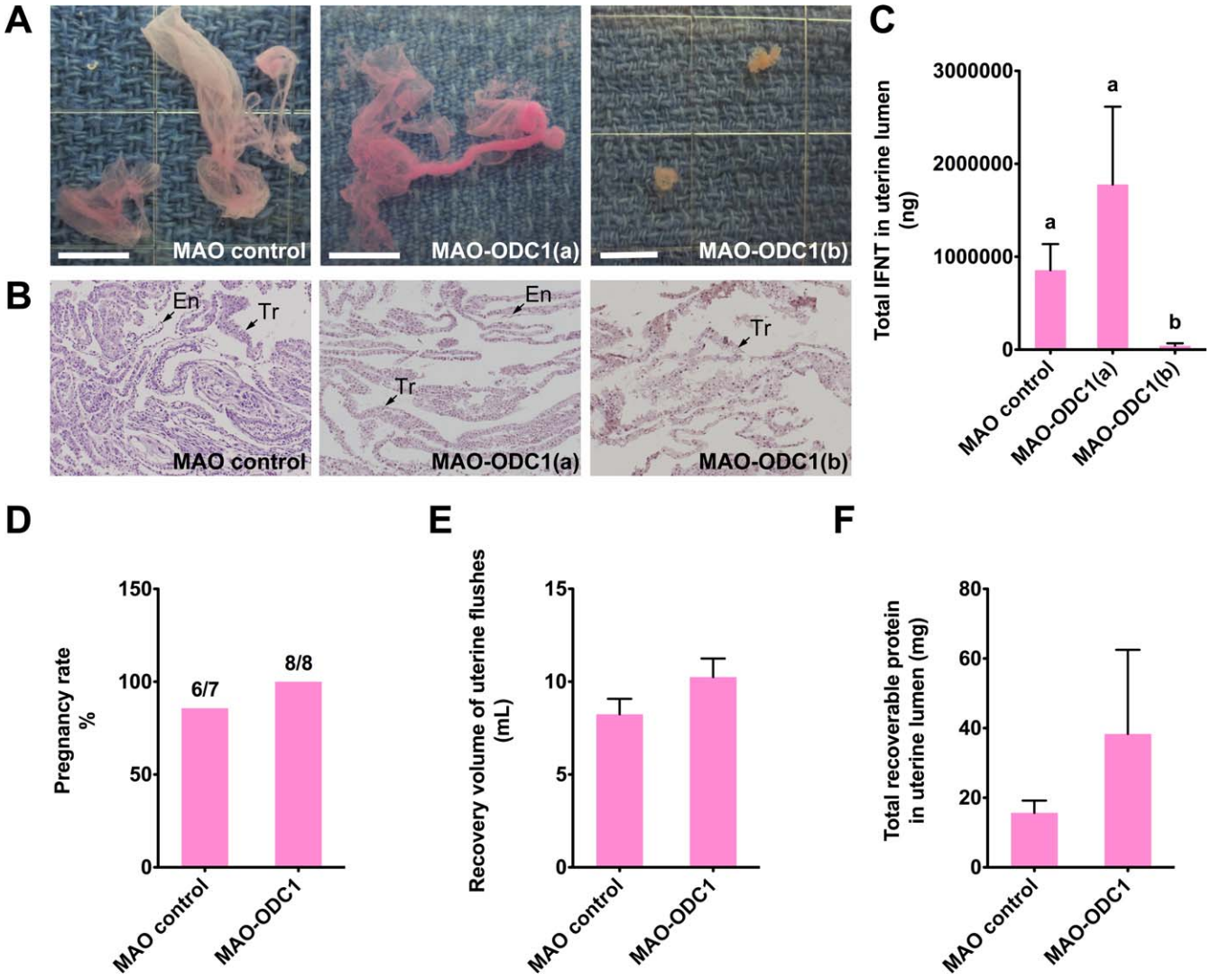

FIG. 1. In vivo knockdown of ODC1 results in two phenotypes of ovine conceptuses based on their morphological and functional development. **A**) Gross morphology of ovine conceptuses on Day 16 of pregnancy indicated that MAO-control conceptuses (n = 6) were morphologically normal and fully elongated to the filamentous form; however, MAO-ODC1 treated conceptuses exhibited two phenotypes: relatively normal morphologically and fully elongated to the filamentous form (n = 4) designated as MAO-ODC1(a) and morphologically abnormal and fragmented with failure to elongate to the filamentous form (n = 4) designated as MAO-ODC1(b). The uptake of 3′-lissamine was not different in the treatment groups, indicating uniform uptake of MAOs. Bar = 0.5 cm. **B**) Histological analyses of conceptuses on Day 16 of pregnancy following staining with hematoxylin and eosin revealed that 1) MAO-control elongated conceptuses (n = 7) had well-organized Tr and extraembryonic En; 2) MAO-ODC1(a) elongated conceptuses (n = 4) had reasonably well-organized Tr and extraembryonic En; and 3) MAO-ODC1(b) conceptuses (n = 4) were not elongated, fragile, and fragmented and lacked extraembryonic En. Tr, trophectoderm; En, endoderm. Width of image field, 900 μm. **C**) The total amount (ng) of interferon tau (IFNT) secreted by conceptuses into the uterine lumen, which served as an index of function of Tr cells, was not different ($P > 0.05$) between MAO-control and MAO-ODC(a) treated conceptuses; however, MAO-ODC1(b) conceptuses secreted less ($P < 0.01$) IFNT. Means with different superscript letters are different ($P < 0.05$). Pregnancy rate (**D**), recovery volume of uterine flushes (**E**), and total recoverable protein in uterine flushes (**F**) were not different among the treatment groups. Data are presented as means and SEM.

compared to either MAO-ODC1(a) or MAO control conceptuses (Fig. 4B).

We next asked whether similar amounts of polyamines in MAO-ODC1(a) and MAO control conceptuses resulted from the conventional arginine to ornithine and putrescine pathway. We found that, as compared with the MAO control, arginine increased about 2-fold ($P < 0.05$) in MAO-ODC1(a) conceptuses but decreased about 50% ($P < 0.05$) in MAO-ODC1(b) conceptuses (Fig. 4D); however, citrulline increased about 2-fold ($P < 0.05$) in MAO-ODC1(a) conceptuses but decreased about 93% ($P < 0.01$) in MAO-ODC1(b) conceptuses (Fig. 4D). There were no significant differences in ornithine in conceptus tissues (Fig. 4D) or arginine in uterine flushings among the treatment groups (Fig. 4C). However, as compared with the MAO control, the amount of ornithine was greater in uterine flushings from MAO-ODC1(a) ($P > 0.05$) and MAO-ODC1(b) ewes ($P < 0.05$; Fig. 4C). Also, citrulline was more abundant ($P < 0.05$) in uterine flushings from both MAO-ODC1(a) and MAO-ODC1(b) ewes (Fig. 4C) due to the increases in NOS3 expression in uteri of MAO-ODC1(a) and MAO-ODC1(b) ewes (Fig. 4E). These results indicate that in vivo knockdown of ODC1 reduces polyamines in the uterine lumen, differentially affects de novo synthesis of polyamines in conceptuses via an alternative metabolic pathway that is

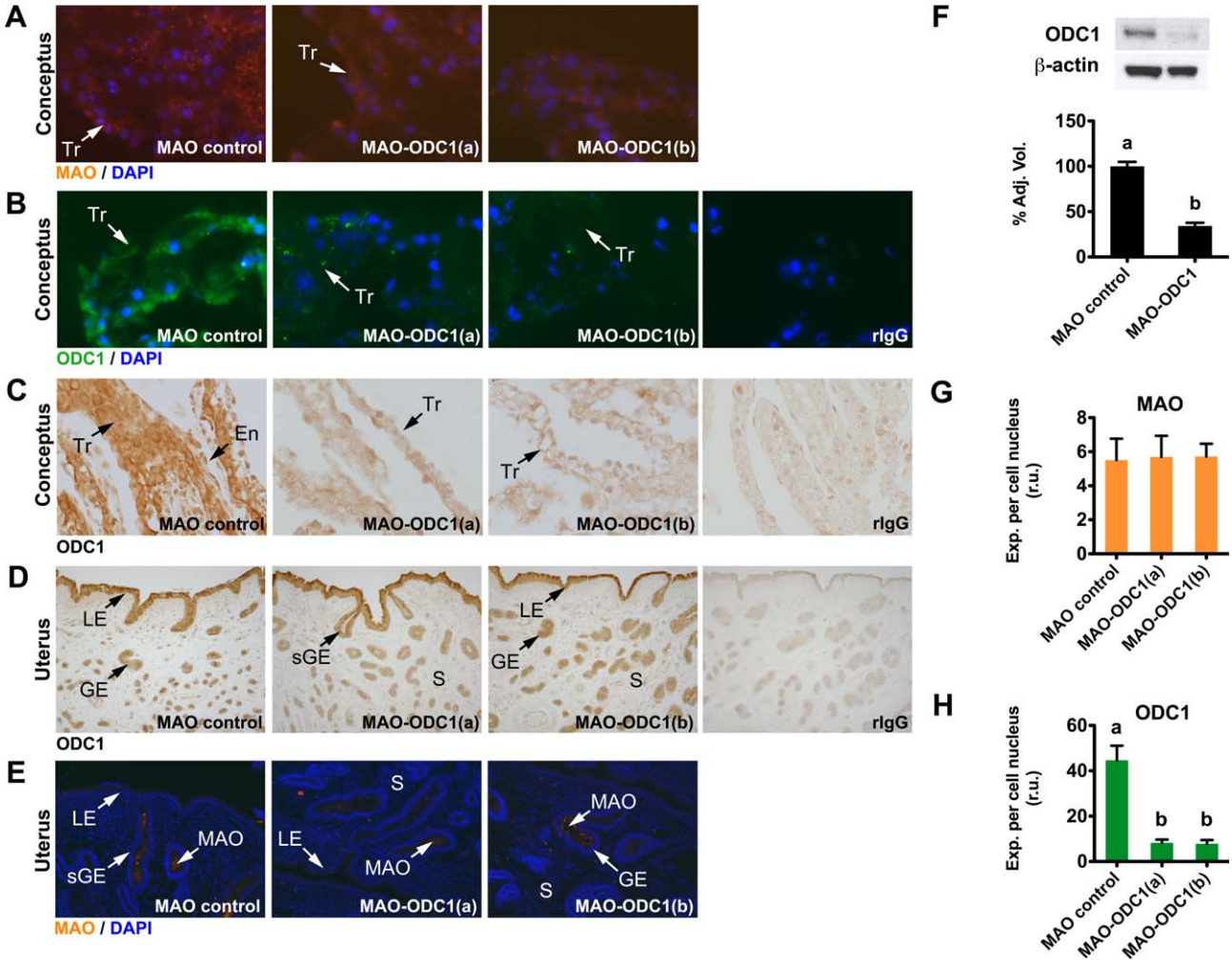

FIG. 2. MAO delivery and knockdown of ODC1 protein by MAO-ODC1 were efficient in ovine conceptuses as well as ovine trophectoderm (oTr) cells, but there was no effect of MAO-ODC1 on ODC1 protein in uterine luminal (LE) and glandular (GE) epithelia. Images (**A**) and quantification (**G**) of delivery efficiency of lissamine-tagged MAOs in MAO control, MAO-ODC1(a), and MAO-ODC1(b) conceptuses confirmed equivalent uptake of MAO by conceptus Tr, but not uterine LE or GE (**D** and **E**). Immunofluorescence analysis (**B**) and immunohistochemical analysis (**C**) as well as quantification of knockdown efficiency (**H**) indicated knockdown of ODC1 protein in MAO-ODC1(a) and MAO-ODC1(b) conceptuses as compared to MAO-control conceptuses. Western blot analysis (**F**) validated knockdown efficiency of ODC1 protein in oTr cell lysates treated with MAO-ODC1 as compared to MAO control when β-actin served as the loading control. Different superscript letters denote significant ($P < 0.05$) differences in abundance of ODC1 protein. Data are presented as means and SEM. MAO-ODC1(a), healthy phenotype; MAO-ODC1(b), unhealthy phenotype; Tr, trophectoderm; En, endoderm; LE, luminal epithelium; GE, glandular epithelium; sGE, superficial glandular epithelium; S, stroma; r.u., relative units. Image width of uteri, 900 μm; image width of conceptuses, 220 μm. In MAO control, n = 6, and in both MAO-ODC1(a) and MAO-ODC1(b), n = 4.

independent of ornithine and ODC1, and also increases the amount of ornithine and citrulline in the uterine lumen.

Knockdown of ODC1 Induced the ADC/AGMAT Pathway, a Rescue Pathway for the Synthesis of Polyamines

We hypothesized that an alternative pathway for production of polyamines accounted for the fact that MAO-ODC1(a) conceptuses elongated and had a normal phenotype. Quantitative RT-PCR analysis indicated that both *ADC* and *AGMAT* transcripts are expressed in Day 16 ovine conceptuses and, importantly, that expression of *ADC* and *AGMAT* mRNAs increased ($P < 0.01$) in MAO-ODC1(a) and MAO-ODC1(b) conceptuses as compared to MAO control (Fig. 5A). No differences in ADC protein were detectable among the three groups of conceptuses (Fig. 5 B and C). However, expression of AGMAT protein increased more than 2-fold ($P < 0.01$) in MAO-ODC1(a), but not MAO-ODC1(b) conceptuses (Fig. 5, B and C). Further high-performance liquid chromatography analyses revealed that, as compared to the MAO control, agmatine increased about 2-fold ($P < 0.05$) in both the conceptuses and uterine lumen of MAO-ODC1(a) conceptuses, but decreased ($P < 0.01$) in MAO-ODC1(b) conceptuses (Fig. 5D). In addition, quantitative immunofluorescence analyses revealed that, as compared to the MAO control, AGMAT protein increased about 2-fold ($P < 0.05$) in uterine LE/sGE and GE of MAO-ODC1(a) ewes (Fig. 6, B and D)., but no difference in ADC protein among uteri of the treatment groups was detected (Fig. 6, A and C). These results indicate that the normal phenotype of MAO-ODC1(a) conceptuses following ODC1 knockdown was associated with the rescue of polyamine synthesis via the ADC/AGMAT pathway in both conceptuses (Fig. 5, B and C) and uteri (Fig. 6)

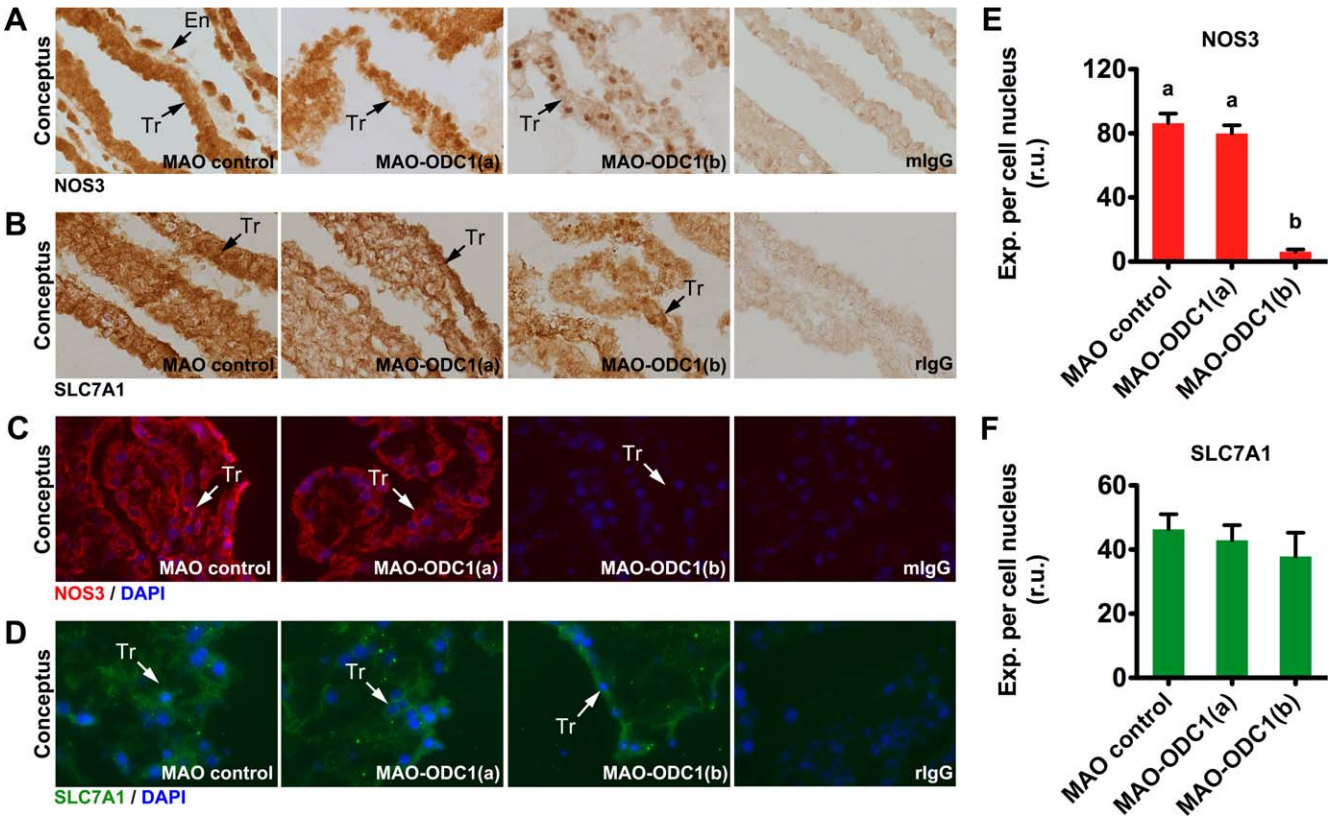

FIG. 3. In vivo knockdown of ODC1 partially suppressed expression of NOS3 protein without affecting expression of SLC7A1 protein in ovine conceptuses. Immunohistochemical analyses (**A** and **B**), immunofluorescence analyses (**C** and **D**), and quantification (**E** and **F**) for NOS3 (**A**, **C**, and **E**) and SLC7A1 (**B**, **D**, and **F**) proteins in MAO control, MAO-ODC1(a), and MAO-ODC1(b) conceptuses on Day 16 of pregnancy revealed a decrease ($P < 0.05$) in NOS3 protein only in MAO-ODC1(b) conceptuses, whereas there were no differences ($P > 0.05$) in SLC7A1 protein among the treatment groups. Sections for immunohistochemical analyses were not counterstained with hematoxylin and eosin, whereas sections for immunofluorescence analyses were stained with DAPI. Mouse IgG (mIgG) or rabbit IgG (rIgG) served as negative controls. Tr, trophectoderm; En, endoderm. Width of field, 220 μm. Different superscript letters denote significant effects of treatment ($P < 0.05$). MAO-ODC1(a), healthy phenotype; MAO-ODC1(b), unhealthy phenotype. Data are presented as means and SEM. For MAO control, n = 6, and for both MAO-ODC1(a) and MAO-ODC1(b), n = 4.

Agmatine Is an Alternative Source for Polyamine Synthesis to Support Ovine Conceptus Growth and Development

To further confirm the hypothesis that agmatine in the uterine lumen and conceptuses provides substrate for polyamine synthesis to support growth and development of conceptuses, we conducted an experiment with untreated ewes having normal growth and development of conceptuses during the peri-implantation period of pregnancy. Ovine conceptuses had the expected morphological changes from tubular to filamentous forms on Days 13 (n = 4), 14 (n = 4), 15 (n = 6), and 16 (n = 6) of pregnancy (Fig. 7A). During that time, total amounts of IFNT secreted by conceptuses into the uterine lumen increase in a quadratic manner with maximum secretion on Day 15 ($P < 0.05$) (Fig. 7B). Polyamines in the uterine lumen decreased linearly from Days 12 to 16 (Fig. 7C). Because we were unable to distinguish the source of polyamines in the uterine lumen as being derived from conceptus or uterus, we determined the abundance of polyamines in extracts of conceptuses from Days 14 to 16. Notably, the amounts of putrescine, spermidine, spermine as well as arginine and ornithine (the conventional source of polyamine synthesis) were greater ($P < 0.05$) in conceptuses from Days 15 to 16 as compared to Day 14 (Fig. 7, D and E). Moreover, there was an increase in agmatine ($P < 0.01$) in conceptuses from Days 15 to 16 as compared to Day 14 (Fig. 7F). Agmatine also increased in the uterine lumen to maximum values on Days 15 to 16 of pregnancy (Fig. 7F). Our systematic investigation on immunohistochemical localization of ADC and AGMAT proteins showed detectable levels of these two enzymes in uterine LE/sGE and GE in both cyclic and pregnant ewes between Days 10 and 16 of pregnancy (Fig. 8, A and B). To our knowledge, the high abundance of agmatine in ovine uterine fluid and conceptus has not been reported for any mammalian tissue. These results indicate that during normal embryonic growth and development in the peri-implantation period of ovine pregnancy, the ODC1-dependent pathway (arginine-ornithine-putrescine) is the dominant pathway for synthesis of polyamines, whereas the ADC/AGMAT-dependent arginine-agmatine-putrescine pathway is a secondary source of polyamines. The concentrations of arginine and ornithine are 10 and 20 times higher, respectively than concentrations of agmatine in normal conceptuses (Fig. 7, E and F). However, in the absence of ODC1, the ADC/AGMAT pathway compensates to provide for de novo synthesis of polyamines required for embryonic survival and development.

DISCUSSION

Successful establishment and maintenance of pregnancy requires appropriate pregnancy recognition signaling from healthy, morphologically well-developed conceptuses [35, 36]. In ruminants, such as sheep, elongation of the spherical blastocyst to tubular and then filamentous forms between Days 12 and 16 of pregnancy is accompanied by increased secretion

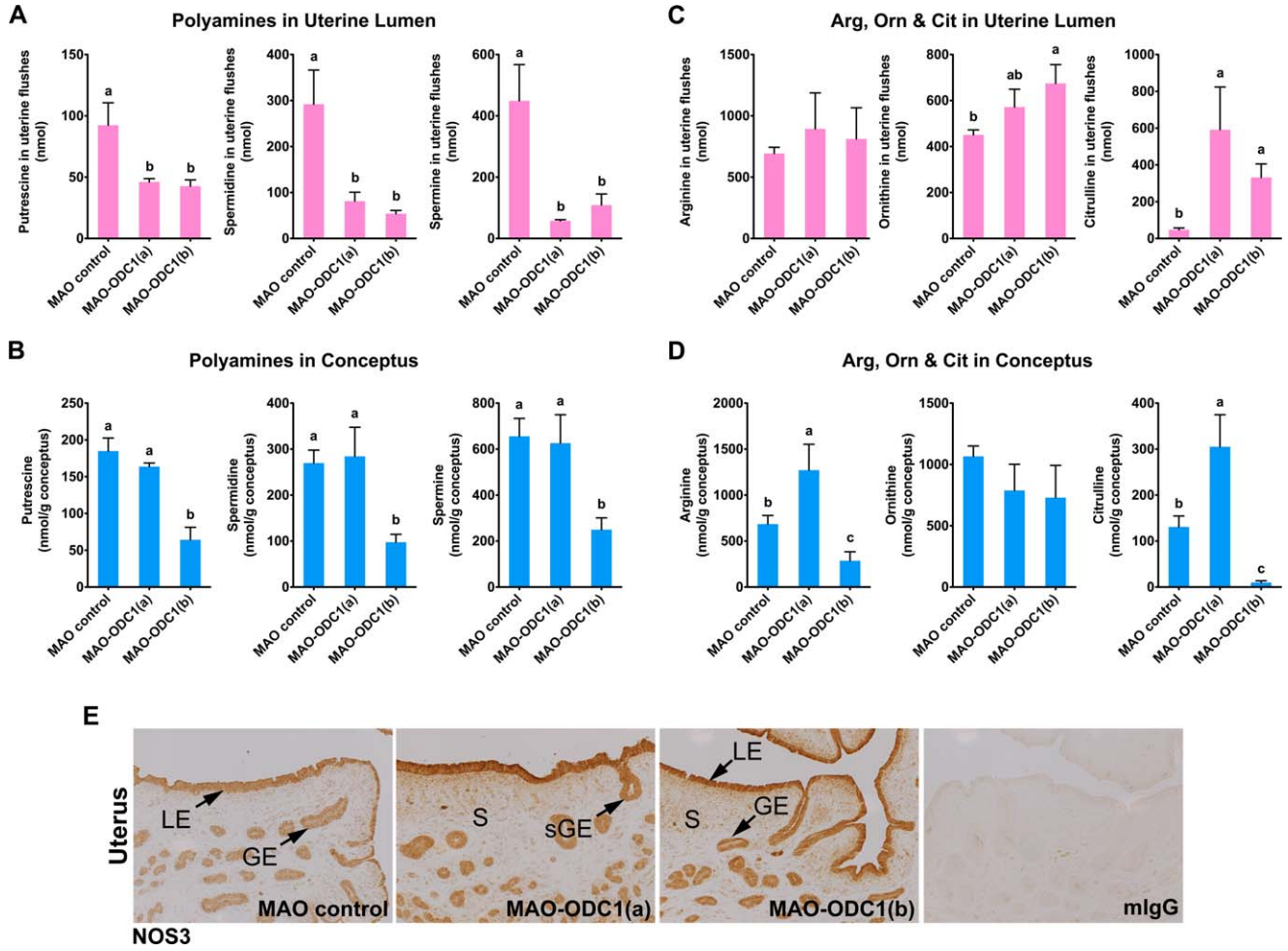

FIG. 4. In vivo knockdown of ODC1 reduced polyamines but increased ornithine and citrulline in the uterine lumen and differentially affected de novo synthesis of polyamines in conceptuses via the conventional conversion of ornithine to putrescine by ODC1. **A**) Total amounts of polyamines (nmol) in uterine flushes were significantly less in MAO-ODC1(a) and MAO-ODC1(b) as compared to MAO-control conceptuses. **B**) The concentrations of polyamines (nmol/g conceptus) in conceptus tissue extracts were not different between MAO control and MAO-ODC1(a) conceptuses, but they were significantly less for MAO-ODC1(b) conceptuses as compared to the other two treatment groups. **C**) Total amounts (nmol) of ornithine (Orn) and citrulline (Cit) were higher in MAO-ODC1(a) and MAO-ODC1(b) ewes as compared to MAO control ewes, whereas total amounts (nmol) of arginine (Arg) in the uterine lumen was not different among the treatment groups. **D**) Concentrations of ornithine (nmol/g conceptus) in conceptus tissue extracts were not different among the treatment groups; however, the concentrations of both arginine and citrulline were less for MAO-ODC1(b) conceptuses and concentrations were actually greater for MAO-ODC1(a) than MAO-control conceptuses. Different superscript letters denote significant differences ($P < 0.05$). Data are presented as means and SEM. **E**) Immunohistochemical analyses of NOS3 protein in uteri of ewes from all the treatment groups revealed increases in NOS3 protein in uteri from both MAO-ODC1(a) and MAO-ODC1(b) as compared to MAO control ewes. Sections were not counterstained with hematoxylin and eosin. Mouse IgG (mIgG) served as the negative control. LE, luminal epithelium; GE, glandular epithelium; sGE, superficial glandular epithelium; S, stroma. Width of field, 900 μm. In MAO control, n = 6, and in both MAO-ODC1(a) and MAO-ODC1(b), n = 4.

FIG. 5. Conceptuses treated with MAO-ODC1 to knockdown ODC1 protein exhibited increased expression of ADC and AGMAT for production of agmatine and polyamines. **A**) Quantitative PCR analyses revealed that the abundance of arginine decarboxylase (ADC) and agmatinase (AGMAT) mRNAs were greater for MAO-ODC1(a) and MAO-ODC1(b) than for MAO-control conceptuses. TUBA is used as internal control gene to normalize the data of ADC and AGMAT, which is shown as relative abundance. **B**) Immunofluorescence analyses indicated greater increases in ADC and AGMAT proteins in MAO-ODC1(a) morphologically and functionally normal conceptuses than in MAO control and MAO-ODC1(b) morphologically and functionally dysfunctional conceptuses. Rabbit IgG (rIgG) served as negative controls. Tr, trophectoderm. Width of field, 220 μm. **C**) Immunofluorescence analysis revealed that the abundance of AGMAT protein was greater for MAO-ODC1(a) than for MAO-control and MAO-ODC1(b) conceptuses, but differences among treatments in abundance of ADC were not significant. r.u., relative units. **D**) The total amount of agmatine (nmol) in uterine flushes was greater for MAO-ODC1(a), as compared to MAO-control and MAO-ODC1(b) conceptuses, which were not different from each other. The concentration of agmatine (nmol/g conceptus) was greatest for MAO-ODC1(a) conceptuses as compared to the other two treatment groups and values were less for MAO-ODC1(b) conceptuses as compared to the other two treatment groups. Different superscript letters denote significant effects of treatment ($P < 0.05$). MAO-ODC1(a), healthy phenotype; MAO-ODC1(b), unhealthy phenotype. Data are presented as means and SEM. In MAO control, n = 6, and in both MAO-ODC1(a) and MAO-ODC1(b), n = 4.

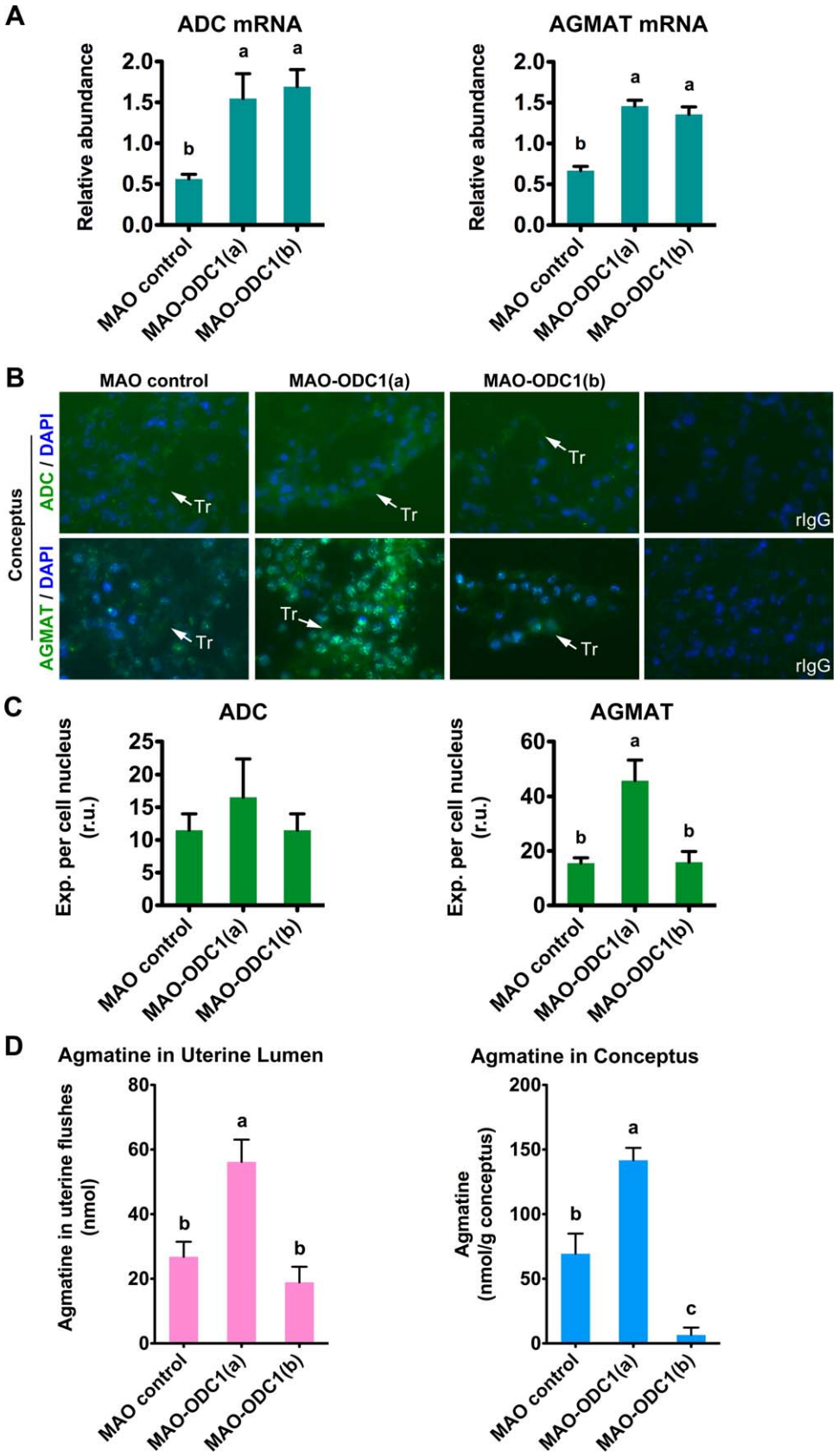

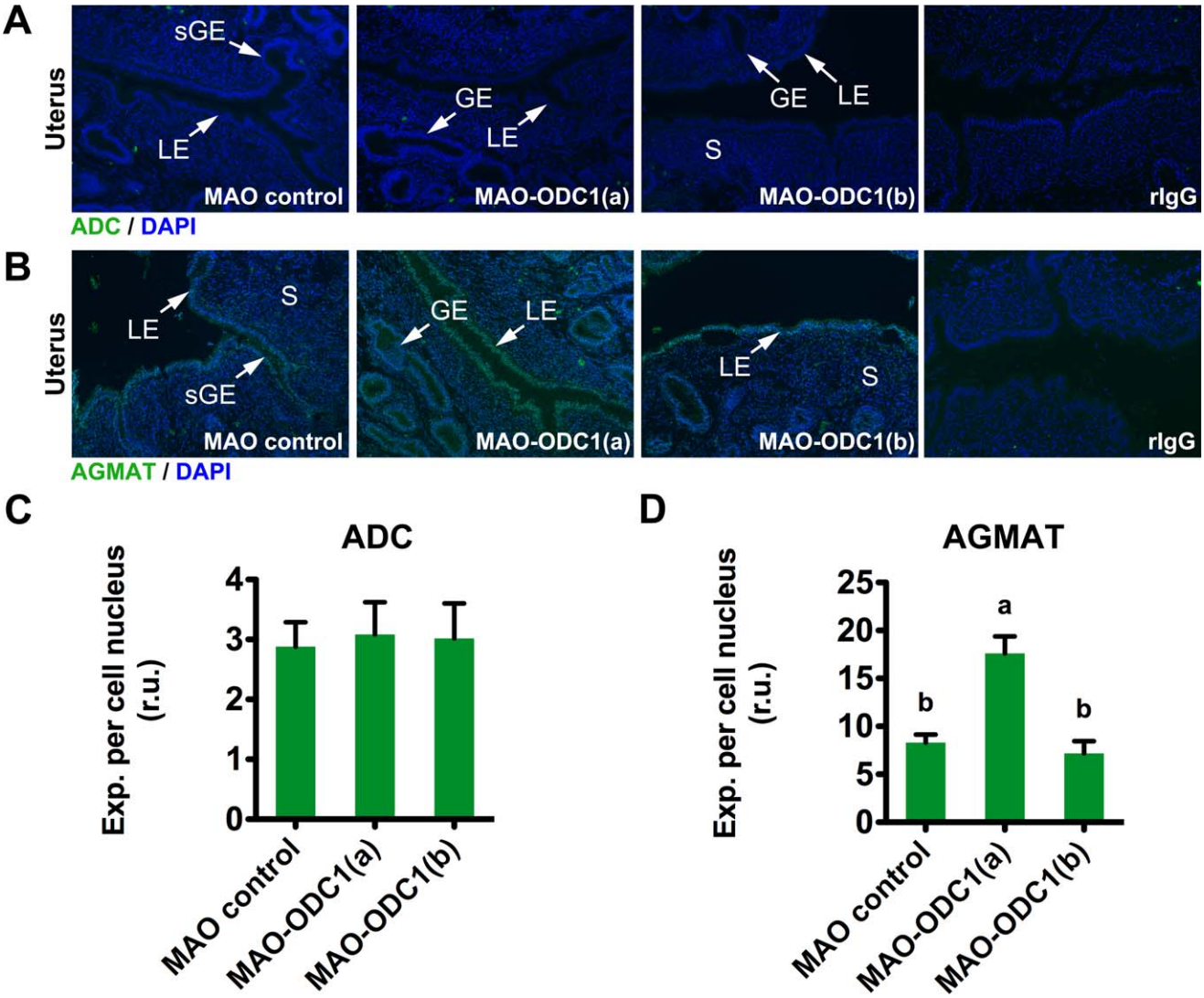

FIG. 6. Uteri treated with MAO-ODC1 to knockdown ODC1 protein in the conceptuses exhibited increased expression of AGMAT but not of ADC proteins for production of polyamines from agmatine. Immunofluorescence analyses (**A** and **B**) as well as the quantification (**C** and **D**) for ADC (**A** and **C**) and AGMAT (**B** and **D**) proteins in MAO control, MAO-ODC1(a), and MAO-ODC1(b) uteri on Day 16 of pregnancy revealed an increase ($P < 0.05$) in AGMAT protein only in MAO-ODC1(a) uteri, whereas there were no differences ($P > 0.05$) in ADC protein among groups. Sections were stained with DAPI. Rabbit IgG (rIgG) served as negative controls. LE, luminal epithelium; GE, glandular epithelium; sGE, superficial glandular epithelium; S, stroma. Width of field, 900 μm. Different superscript letters denote significant effects of treatment ($P < 0.05$). MAO-ODC1(a), healthy phenotype; MAO-ODC1(b), unhealthy phenotype. Data are presented as means and SEM. In MAO control, n = 6, and in both MAO-ODC1(a) and MAO-ODC1(b), n = 4.

of IFNT that signals pregnancy recognition and, in concert with progesterone, increases expression of key genes in uterine LE and sGE for transport of nutrients such as arginine into the uterine lumen [37–41]. Arginine, a nutritionally essential amino acid for growth and development of the conceptus [40, 42, 43], increases 13-fold in the uterine lumen [4] between Days 10 and 15 of pregnancy to support conceptus growth and development as a precursor for production of both NO and polyamines [6, 17, 44]. The in vivo functions of cellular polyamines in the conceptus and uterus are poorly understood [19, 45, 46]. Therefore, we wished to gain insight into the role of ODC1 in the de novo biosynthesis of putrescine in the ovine conceptus using a morpholino loss-of-function approach in utero to knockdown ODC1 protein only in conceptus Tr [47, 48].

Results of our study provide in vivo physiological evidence that polyamines are critical for conceptus development and that the ADC/AGMAT pathway in mammalian conceptuses can serve as a functional compensatory metabolic pathway for production of polyamines in the absence of ODC1. In the absence of ODC1 protein, half of the conceptuses were normal. This MAO-ODC1(a) phenotype appears to be due to ADC converting arginine to agmatine and a compensatory increase in AGMAT protein that resulted in an increase in putrescine and other polyamines in the MAO-ODC1(a) conceptuses. However, conceptuses that did not exhibit an increase in expression of AGMAT protein in the absence of ODC1 failed to develop normally, and they secreted significantly less IFNT. These results support our hypothesis that in the absence of ODC1, agmatine derived via the ADC/AGMAT pathway in the uterine lumen and conceptuses allows de novo synthesis of polyamines required for survival and development of the conceptus. It is not clear if the ADC/AGMAT pathway is unique to ovine conceptuses because *odc1* null mouse embryos die at the gastrulation stage and mink blastocysts fail to

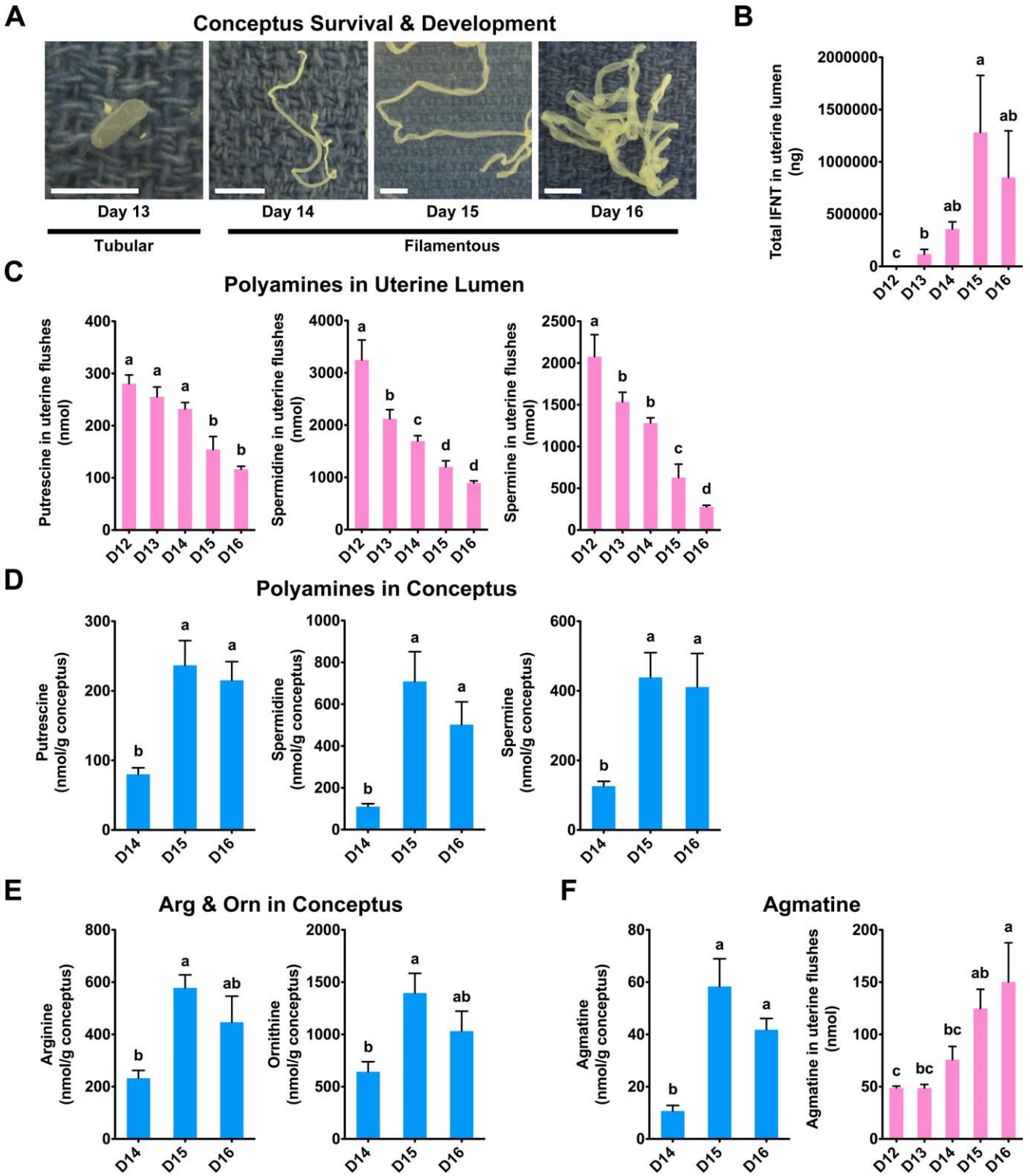

FIG. 7. During the peri-implantation period of pregnancy in ewes, there are changes in the abundance of polyamines, agmatine, ornithine, and arginine in uterine flushings and conceptuses as they transition from tubular to fully elongated conceptuses and secrete interferon tau (IFNT) to signal pregnancy recognition and to act in concert with progesterone to increase transport of nutrients into the uterine lumen. **A**) Ovine conceptuses undergo a morphological transition from the tubular (Day 13) to elongated filamentous forms between Days 14 and 16 of pregnancy. Bar = 0.5 cm. **B**) The increase in total amount (ng) of IFNT secreted by conceptuses and recovered in uterine flushings between Days 12 and 16 of pregnancy signals pregnancy recognition. **C**) There is a decrease in total amounts of polyamines (nmol) in uterine flushes from Day 12 to Day 16 of pregnancy. **D**) The concentrations of polyamines (nmol/g conceptus) in conceptuses increase from Days 14 to 16 of pregnancy. **E**) Concentrations of arginine and ornithine (nmol/g conceptus) increase in conceptuses from Days 14 to 16 of pregnancy. **F**) Concentration of agmatine increase in conceptuses (nmol/g) and total recoverable agmatine (nmol) increases in uterine flushes during the peri-implantation period of pregnancy. Means with different superscript letters are significantly different ($P < 0.05$). Data are presented as means and SEM. For Days 12–16 of pregnancy, n = 3, 4, 4, 6, and 6, respectively.

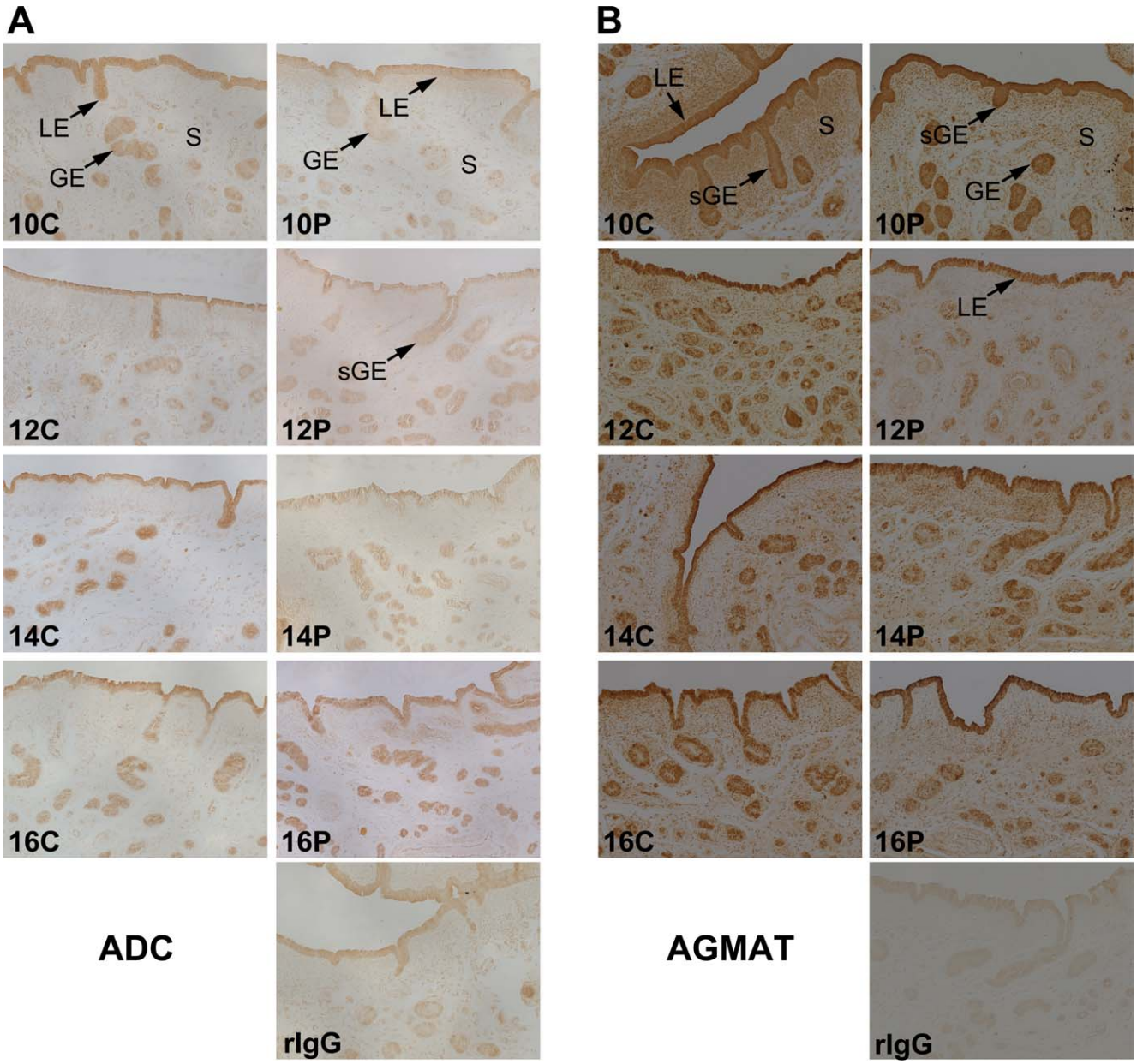

FIG. 8. Immunohistochemical localization of ADC and AGMAT proteins in uteri of cyclic (C) and pregnant (P) ewes. ADC protein (**A**) was weakly detectable, whereas AGMAT protein (**B**) was strongly expressed in uterine LE/sGE and GE of both cyclic and pregnant ewes between Days 10 and 16 of pregnancy. LE, luminal epithelium; GE, glandular epithelium; sGE, superficial glandular epithelium; S, stroma. Width of field, 900 μm; n = 4 per day and status.

undergo expansion and implantation if arginase, which converts arginine to ornithine, is inhibited [22].

Based on evidence from the literature that the absence or suppression of ODC1 results in failure of conceptus development, we were surprised to find that ODC1 knockdown in ovine conceptus Tr did not completely disrupt development of the conceptuses, but generated two phenotypes that we designated MAO-ODC1(a) if they were rescued and MAO-ODC1(b) if they were severely retarded in development as compared to MAO control conceptuses. These two phenotypes were observed in two replicates of ODC1-MAO treatment of ovine conceptuses in 2011 (four normal and four retarded) and 2012 (four normal and four retarded). After confirming MAO delivery and knockdown of ODC1 protein in conceptuses, we considered alternative pathways for de novo biosynthesis of polyamines from arginine and found reports on the ADC/AGMAT pathway for synthesis of polyamines in nonmammalian organisms including microbes [49], plants [50], and pathogens [51] as well as nervous tissue [24] and liver [23] of rats. In rat brain, arginine is converted to agmatine by ADC and stored in neuronal cells where it functions as a putative neuromodulator [52]. However, there are no published reports of expression of ADC/AGMAT genes in the mammalian reproductive tract or conceptus. Nevertheless, we examined expression of *ADC* and *AGMAT* mRNAs and proteins in the ovine conceptus and found expression of ADC and AGMAT in the ovine uterus (Fig. 8) and conceptus (Fig. 5B). Furthermore, the expression of these enzymes was up-regulated in the absence of ODC1 as an alternative source for polyamine biosynthesis and rescue of conceptus development. Quantitative immunofluorescence results indicated the compensatory increase of AGMAT protein in MAO-ODC1(a), but not MAO-

ODC1(b) conceptuses. In addition, the increase in the abundance of agmatine in the uterine lumen and in conceptus tissues confirmed that agmatine metabolism via ADC/AGMAT is an alternative source of polyamines to support development of MAO-ODC1(a) conceptuses, but not MAO-ODC1(b) conceptuses.

We were also interested in effects of ODC1 knockdown on expression of NOS3 protein because: 1) arginine catabolism includes not only polyamines via ODC1, but also NO production via NOS3; and 2) polyamines exist as complexes with DNA, RNA, and ATP with the largest portion being polyamine-RNA complexes that regulate global mRNA translation [13, 53]. The result suggested the existence of cross-talk between NOS3 and ODC1 (via polyamine levels) in conceptuses. NOS3 is the major enzyme to catabolize arginine into citrulline and NO in ovine conceptuses. Our results indicated that NOS3 is less abundant in MAO-ODC1(b) conceptuses as compared to MAO-ODC1(a) and MAO control conceptuses, but there was no difference in NOS3 abundance between MAO-ODC1(a) and MAO control conceptuses (Fig. 3, A and C). We speculate that the lower abundance of NOS3 protein in MAO-ODC1(b) is due to the lower abundance of polyamines that form polyamine-RNA complexes that decrease translation of *NOS3* mRNA, or that there is a preferential sparing of arginine for synthesis of polyamines because arginine and agmatine are lowest in MAO-ODC1(b) conceptuses (Figs. 4D and 5D). This is further confirmed by the abundance of citrulline, the product of NOS3, which was decreased significantly in MAO-ODC1(b) compared with MAO-ODC1(a) and MAO control (Fig. 4D). Interestingly, citrulline also increased significantly in MAO-ODC1(a) compared with MAO control (Fig. 4D). This might be due to 1) increased enzymatic activity of NOS3 or 2) increased conversion of ornithine to citrulline via ornithine carbamoyltransferase (OCT). This may also explain why there was no accumulation of ornithine, the substrate of ODC1 in MAO-ODC1(a) conceptuses (Fig. 4D).

Next, we determined whether the abundance of polyamines in the uterine lumen and conceptuses were affected differentially by ODC1 knockdown. The significant decrease in polyamines in the uterine lumen of both MAO-ODC1(a) and MAO-ODC1(b) treatment groups indicated the essential role of ODC1, the rate-limiting enzyme for de novo synthesis of polyamines. However, it is also imperative to assess effects of ODC1 knockdown on abundance of polyamines in conceptus tissues because uterine LE/GE and conceptuses can produce and/or transport polyamines. Our results on the abundance of polyamines in conceptuses provided insight into how MAO-ODC1(a) conceptuses were rescued in that they had similar amounts of polyamines as MAO control conceptuses, whereas MAO-ODC1(b) conceptuses were deficient in polyamines. Furthermore, arginine was more abundant in MAO-ODC1(a) than MAO-ODC1(b) as well as MAO control conceptuses, suggesting that arginine transport from uterine LE/GE to uterine lumen to conceptuses Tr is different among the MAO control, MAO-ODC1(a), and MAO-ODC1(b) phenotypes following ODC1 knockdown. It is also possible that there are differences among MAO-ODC1(a) and MAO-ODC1(b) conceptus phenotypes in the efficiencies for biosynthesis of arginine from other amino acids (e.g., glutamine, glutamate, and proline) [42]. However, there were no differences in SLC7A1 protein among conceptuses of the treatment groups (Fig. 3, B and D), suggesting that arginine is being synthesized from other amino acids. The abundance of ornithine, the substrate for ODC1, was not affected by the conceptus phenotype.

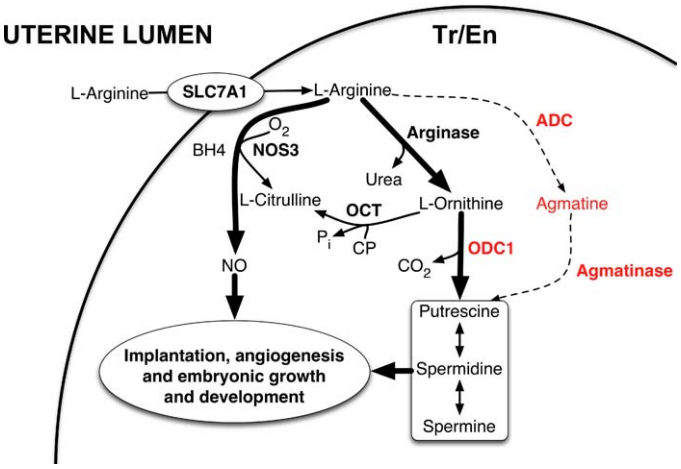

FIG. 9. Schematic pathway whereby ADC and AGMAT participate in compensatory de novo biosynthesis of polyamines to support growth and development of the conceptus. De novo biosynthesis of polyamines in conceptuses is primarily via the conventional ODC1-dependent metabolic pathway (arginine-ornithine-putrescine). However, the ADC/AGMAT-dependent arginine-agmatine-putrescine pathway also exists in ovine conceptuses. In the absence of ODC1 protein, the expression of ADC and AGMAT increase to provide adequate amounts of polyamines for support of conceptus development. However, there appears to be considerable among-conceptus variation in the degree of activation of the ADC/AGMAT pathway as noted in the present study. Changes in abundance of agmatine in the uterine lumen may also reflect multiple functional roles of agmatine within the pregnant uterus. OCT, ornithine carbamoyltransferase; CP, carbamoyl phosphate.

Results from our in vivo study of consequences of ODC1 knockdown clearly indicate that conceptus development is disrupted when the abundance of polyamines is insufficient. In vitro studies revealed the requirement for polyamines in initiation of mRNA translation and cell proliferation in mammalian cells [19, 54]. It is quite remarkable that some conceptuses with ODC1 knockdown were rescued from being developmentally abnormal based on the expression of AGMAT, perhaps due to variations among conceptuses at the genomic or epigenomic levels. To confirm that agmatine metabolism occurs during the course of normal conceptus development, we investigated temporal patterns of change in abundance of polyamines, selected amino acids, and agmatine in the uterine lumen and conceptuses during the peri-implantation period of pregnancy when ewes received no treatments. The results indicated that 1) the requirement for polyamines by conceptuses increases significantly as they become more developed and take up increasing amounts of polyamines from the uterine lumen (Fig. 7C); 2) the abundance of polyamines increases in healthy developing conceptuses (Fig. 7D); 3) de novo biosynthesis of polyamines in conceptuses is mainly via the conventional ODC1-dependent pathway (arginine-ornithine-putrescine) (Figs. 7E and 9); and 4) activity of the ADC/AGMAT-dependent pathway (arginine-agmatine-putrescine) is less active than the ODC1-pathway for the synthesis of polyamines (Figs. 7F, 8, and 9) [6]. In addition, agmatine increased in the uterine lumen and in the conceptus between Days 12 and 16 of the peri-implantation period of pregnancy (Fig. 7F). Also, ADC and AGMAT remain detectable in uteri of cyclic and pregnant ewes from Days 10 to 16 after onset of estrus (Fig. 8). Thus, agmatine may serve as a substrate for production of putrescine or it may have other functional roles with respect to uterine functions and/or conceptus development.

In summary, physiological levels of polyamines are essential for embryonic survival, growth, and development (Fig. 9). In vivo knockdown of ODC1, the classical key enzyme for putrescine biosynthesis, results in variable phenotypes based on their ability to activate the alternative ADC/AGMAT pathway for synthesis of polyamines. Future studies will address the physiological role of agmatine in reproductive functions and conceptus development as well as the underlying mechanism for induction of the ADC/AGMAT pathway to increase the abundance of both agmatine and polyamines vital to survival, growth, and development of the mammalian conceptus.

ACKNOWLEDGMENT

The contributions of graduate students and postdoctoral fellows from the Laboratory of Uterine Biology and Pregnancy are gratefully acknowledged as is the assistance of Messrs. Kendrick Leblanc, Colt Sharpton, and Caleb Wendt for management of the experimental animals.

REFERENCES

1. Bazer FW. Uterine protein secretions: relationship to development of the conceptus. J Anim Sci 1975; 41:1376–1382.
2. Spencer TE, Bazer FW. Uterine and placental factors regulating conceptus growth in domestic animals. J Anim Sci 2004; 82(E-Suppl):E4–E13.
3. Wu G, Bazer FW, Cudd TA, Meininger CJ, Spencer TE. Maternal nutrition and fetal development. J Nutr 2004; 134:2169–2172.
4. Gao H, Wu G, Spencer TE, Johnson GA, Li X, Bazer FW. Select nutrients in the ovine uterine lumen. I. Amino acids, glucose, and ions in uterine lumenal flushings of cyclic and pregnant ewes. Biol Reprod 2009; 80: 86–93.
5. Gao H, Wu G, Spencer TE, Johnson GA, Bazer FW. Select nutrients in the ovine uterine lumen. III. Cationic amino acid transporters in the ovine uterus and peri-implantation conceptuses. Biol Reprod 2009; 80:602–609.
6. Gao H, Wu G, Spencer TE, Johnson GA, Bazer FW. Select nutrients in the ovine uterine lumen. V. Nitric oxide synthase, GTP cyclohydrolase, and ornithine decarboxylase in ovine uteri and peri-implantation conceptuses. Biol Reprod 2009; 81:67–76.
7. Gouge RC, Marshburn P, Gordon BE, Nunley W, Huet-Hudson YM. Nitric oxide as a regulator of embryonic development. Biol Reprod 1998; 58:875–879.
8. Sengoku K, Takuma N, Horikawa M, Tsuchiya K, Komori H, Sharifa D, Tamate K, Ishikawa M. Requirement of nitric oxide for murine oocyte maturation, embryo development, and trophoblast outgrowth in vitro. Mol Reprod Dev 2001; 58:262–268.
9. Bird IM, Zhang L, Magness RR. Possible mechanisms underlying pregnancy-induced changes in uterine artery endothelial function. Am J Physiol Regul Integr Comp Physiol 2003; 284:R245–R258.
10. Wu G, Bazer FW, Wallace JM, Spencer TE. Board-invited review: intrauterine growth retardation: implications for the animal sciences. J Anim Sci 2006; 84:2316–2337.
11. Heby O. DNA methylation and polyamines in embryonic development and cancer. Int J Dev Biol 1995; 39:737–757.
12. Wallace HM, Fraser AV, Hughes A. A perspective of polyamine metabolism. Biochem J 2003; 376:1–14.
13. Igarashi K, Kashiwagi K. Modulation of cellular function by polyamines. Int J Biochem Cell Biol 2010; 42:39–51.
14. Chattopadhyay MK, Tabor CW, Tabor H. Polyamines protect *Escherichia coli* cells from the toxic effect of oxygen. Proc Natl Acad Sci U S A 2003; 100:2261–2265.
15. Nishimura K, Murozumi K, Shirahata A, Park MH, Kashiwagi K, Igarashi K. Independent roles of eIF5A and polyamines in cell proliferation. Biochem J 2005; 385:779–785.
16. Maeda T, Wakasawa T, Shima Y, Tsuboi I, Aizawa S, Tamai I. Role of polyamines derived from arginine in differentiation and proliferation of human blood cells. Biol Pharm Bull 2006; 29:234–239.
17. Kim JY, Burghardt RC, Wu G, Johnson GA, Spencer TE, Bazer FW. Select nutrients in the ovine uterine lumen. VIII. Arginine stimulates proliferation of ovine trophectoderm cells through MTOR-RPS6K-RPS6 signaling cascade and synthesis of nitric oxide and polyamines. Biol Reprod 2011; 84:70–78.
18. Igarashi K, Kashiwagi K. Polyamines: mysterious modulators of cellular functions. Biochem Biophys Res Commun 2000; 271:559–564.
19. Mandal S, Mandal A, Johansson HE, Orjalo AV, Park MH. Depletion of cellular polyamines, spermidine and spermine, causes a total arrest in translation and growth in mammalian cells. Proc Natl Acad Sci U S A 2013; 110:2169–2174.
20. Lefevre PL, Palin MF, Beaudry D, Dobias-Goff M, Desmarais JA, Llerena VE, Murphy BD. Uterine signaling at the emergence of the embryo from obligate diapause. Am J Physiol Endocrinol Metab 2011; 300:E800–E808.
21. Lefevre PL, Palin MF, Chen G, Turecki G, Murphy BD. Polyamines are implicated in the emergence of the embryo from obligate diapause. Endocrinology 2011; 152:1627–1639.
22. Lefevre PL, Palin MF, Murphy BD. Polyamines on the reproductive landscape. Endocr Rev 2011; 32:694–712.
23. Horyn O, Luhovyy B, Lazarow A, Daikhin Y, Nissim I, Yudkoff M, Nissim I. Biosynthesis of agmatine in isolated mitochondria and perfused rat liver: studies with 15N-labelled arginine. Biochem J 2005; 388: 419–425.
24. Iyo AH, Zhu MY, Ordway GA, Regunathan S. Expression of arginine decarboxylase in brain regions and neuronal cells. J Neurochem 2006; 96: 1042–1050.
25. GeneCardV3 [Internet]. Rehovot, Israel: Crown Human Genome Center, Department of Molecular Genetics, The Weizmann Institute of Science. http://www.genecards.org/. Accessed 15 March 2014.
26. Dunlap KA, Palmarini M, Varela M, Burghardt RC, Hayashi K, Farmer JL, Spencer TE. Endogenous retroviruses regulate periimplantation placental growth and differentiation. Proc Natl Acad Sci U S A 2006; 103:14390–14395.
27. Spencer TE, Bartol FF, Bazer FW, Johnson GA, Joyce MM. Identification and characterization of glycosylation-dependent cell adhesion molecule 1-like protein expression in the ovine uterus. Biol Reprod 1999; 60:241–250.
28. Antoniazzi AQ, Webb BT, Romero JJ, Ashley RL, Smirnova NP, Henkes LE, Bott RC, Oliveira JF, Niswender GD, Bazer FW, Hansen TR. Endocrine delivery of interferon tau protects the corpus luteum from prostaglandin F2 alpha-induced luteolysis in ewes. Biol Reprod 2013; 88: 144.
29. Kim JY, Burghardt RC, Wu G, Johnson GA, Spencer TE, Bazer FW. Select nutrients in the ovine uterine lumen. VII. Effects of arginine, leucine, glutamine, and glucose on trophectoderm cell signaling, proliferation, and migration. Biol Reprod 2011; 84:62–69.
30. Kim J, Song G, Wu G, Bazer FW. Functional roles of fructose. Proc Natl Acad Sci U S A 2012; 109:E1619–E1628.
31. Arqués O, Chicote I, Tenbaum S, Puig I, G, Palmer H. Standardized relative quantification of immunofluorescence tissue staining. Protocol Exchange 2012. DOI:10.1038/protex.2012.008.
32. Wu G, Bazer FW, Hu J, Johnson GA, Spencer TE. Polyamine synthesis from proline in the developing porcine placenta. Biol Reprod 2005; 72: 842–850.
33. Wu G, Flynn NE, Knabe DA. Enhanced intestinal synthesis of polyamines from proline in cortisol-treated piglets. Am J Physiol Endocrinol Metab 2000; 279:E395–E402.
34. Wu G, Davis PK, Flynn NE, Knabe DA, Davidson JT. Endogenous synthesis of arginine plays an important role in maintaining arginine homeostasis in postweaning growing pigs. J Nutr 1997; 127:2342–2349.
35. Spencer TE, Ott TL, Bazer FW. tau-Interferon: pregnancy recognition signal in ruminants.Proc Soc Exp Biol Med 1996; 213:215–229.
36. Bazer FW, Spencer TE, Ott TL. Interferon tau: a novel pregnancy recognition signal. Am J Reprod Immunol 1997; 37:412–420.
37. Dorniak P, Bazer FW, Spencer TE. Prostaglandins regulate conceptus elongation and mediate effects of interferon tau on the ovine uterine endometrium. Biol Reprod 2011; 84:1119–1127.
38. Dorniak P, Bazer FW, Spencer TE. Physiology and Endocrinology Symposium: biological role of interferon tau in endometrial function and conceptus elongation. J Anim Sci 2013; 91:1627–1638.
39. Dorniak P, Welsh TH Jr, Bazer FW, Spencer TE. Cortisol and interferon tau regulation of endometrial function and conceptus development in female sheep. Endocrinology 2013; 154:931–941.
40. Bazer FW, Kim J, Ka H, Johnson GA, Wu G, Song G. Select nutrients in the uterine lumen of sheep and pigs affect conceptus development. J Reprod Dev 2012; 58:180–188.
41. Bazer FW, Kim J, Song G, Ka H, Tekwe CD, Wu G. Select nutrients, progesterone, and interferon tau affect conceptus metabolism and development. Ann N Y Acad Sci 2012; 1271:88–96.
42. Wu G, Bazer FW, Davis TA, Kim SW, Li P, Marc Rhoads J, Carey Satterfield M, Smith SB, Spencer TE, Yin Y. Arginine metabolism and nutrition in growth, health and disease. Amino Acids 2009; 37:153–168.
43. Bazer FW, Wu G, Johnson GA, Kim J, Song G. Uterine histotroph and conceptus development: select nutrients and secreted phosphoprotein 1 affect mechanistic target of rapamycin cell signaling in ewes. Biol Reprod 2011; 85:1094–1107.

44. Kim J, Burghardt RC, Wu G, Johnson GA, Spencer TE, Bazer FW. Select nutrients in the ovine uterine lumen. IX. Differential effects of arginine, leucine, glutamine, and glucose on interferon tau, ornithine decarboxylase, and nitric oxide synthase in the ovine conceptus. Biol Reprod 2011; 84: 1139–1147.
45. Kusano T, Berberich T, Tateda C, Takahashi Y. Polyamines: essential factors for growth and survival. Planta 2008; 228:367–381.
46. Persson L. Polyamine homoeostasis. Essays Biochem 2009; 46:11–24.
47. Pegg AE. Recent advances in the biochemistry of polyamines in eukaryotes. Biochem J 1986; 234:249–262.
48. Hillary RA, Pegg AE. Decarboxylases involved in polyamine biosynthesis and their inactivation by nitric oxide. Biochim Biophys Acta 2003; 1647: 161–166.
49. Nakada Y, Itoh Y. Identification of the putrescine biosynthetic genes in *Pseudomonas aeruginosa* and characterization of agmatine deiminase and N-carbamoylputrescine amidohydrolase of the arginine decarboxylase pathway. Microbiology 2003; 149:707–714.
50. Illingworth C, Mayer MJ, Elliott K, Hanfrey C, Walton NJ, Michael AJ. The diverse bacterial origins of the Arabidopsis polyamine biosynthetic pathway. FEBS Lett 2003; 549:26–30.
51. Keithly JS, Zhu G, Upton SJ, Woods KM, Martinez MP, Yarlett N. Polyamine biosynthesis in *Cryptosporidium parvum* and its implications for chemotherapy. Mol Biochem Parasitol 1997; 88:35–42.
52. Bernstein HG, Derst C, Stich C, Pruss H, Peters D, Krauss M, Bogerts B, Veh RW, Laube G. The agmatine-degrading enzyme agmatinase: a key to agmatine signaling in rat and human brain? Amino Acids 2011; 40: 453–465.
53. Landau G, Bercovich Z, Park MH, Kahana C. The role of polyamines in supporting growth of mammalian cells is mediated through their requirement for translation initiation and elongation. J Biol Chem 2010; 285:12474–12481.
54. Ogasawara T, Ito K, Igarashi K. Effect of polyamines on globin synthesis in a rabbit reticulocyte polyamine-free protein synthetic system. J Biochem 1989; 105:164–167.